

Spectroscopic and Potentiometric Characterization of Oxovanadium(IV) Complexes Formed by 3-Hydroxy-4-Pyridinones. Rationalization of the Influence of Basicity and Electronic Structure of the Ligand on the Properties of $V^{IV}O$ Species in Aqueous Solution

Maria Rangel, Andreia Leite, and M. João Amorim

REQUIMTE, Instituto de Ciências Biomédicas de Abel Salazar, Universidade do Porto, Largo Abel Salazar 2, 4099-003 Porto, Portugal

Eugenio Garribba* and Giovanni Micera*

Dipartimento di Chimica, Università degli Studi di Sassari, Via Vienna 2, I-07100 Sassari, Italy

Elzbieta Lodyga-Chruscinska

Institute of General Food Chemistry, Technical University of Lodz, ulice Stefanowskiego 4/10, PL-90924 Lodz, Poland

Received April 3, 2006

Aqueous solution studies regarding the identification and characterization of complexes formed by the $V^{IV}O$ ion and 11 3-hydroxy-4-pyridinone derivatives have been performed using EPR and UV/vis spectroscopic techniques. For the three ligands (HL) adequately soluble in water (1-methyl-3-hydroxy-4-pyridinone, 1-methyl-2-ethyl-3-hydroxy-4-pyridinone, and 1,2-diethyl-3-hydroxy-4-pyridinone), potentiometric titrations were performed; the results are consistent with the formation of $[V^{IV}OL]^+$, $[V^{IV}OL_2]$, $[V^{IV}OL_2H_{-1}]^-$, $[(V^{IV}O)_2L_2H_{-2}]$, and $[V^{IV}L_3]^+$ species. Bis chelated complexes are characterized by a cis–trans isomerism, the trans isomer being strongly favored with respect to the cis arrangement. Tris chelated non-oxo V^{IV} species were prepared in CH_3COOH ; their spectroscopic features point to a d_2 ground state and a geometry intermediate between an octahedron and a trigonal prism, related to the steric requirements of the substituent on the carbon atom in position 2 of the pyridinone ring. Four new solid derivatives, $[V^{IV}O(1,2\text{-diethyl-3-hydroxy-4-pyridinonato})_2]$, $[V^{IV}O(1\text{-}(p\text{-tolyl})\text{-2-ethyl-3-hydroxy-4-pyridinonato})_2]$, $[V^{IV}O(1\text{-}(p\text{-}(n\text{-butyl})\text{phenyl})\text{-2-ethyl-3-hydroxy-4-pyridinonato})_2]$, and $[V^{IV}O(1\text{-}(p\text{-}(n\text{-hexyl})\text{phenyl})\text{-2-ethyl-3-hydroxy-4-pyridinonato})_2]$, were isolated and characterized; they exhibited a five-coordinate geometry close to square-pyramid. A criterion for establishing the degree of distortion toward the trigonal-bipyramid on the basis of the electronic absorption spectra is provided. Relationships between the pK_a of the –OH group in position 3 of the ring and (i) $\log K$ of mono and bis chelated complexes, (ii) pK of the water molecule in $cis\text{-}[V^{IV}OL_2(H_2O)]$, (iii) $\log K$ of tris chelated species $[V^{IV}L_3]^+$, and (iv) ^{51}V hyperfine coupling constant (A_z) have been established and discussed for a number of pyrone, pyridinone, and catechol ligands. The results are rationalized by assuming for pyridinones an electronic structure intermediate between that of pyrones and catechols. The relationships are valuable to the understanding of the behavior of $V^{IV}O$ species in aqueous solution.

Introduction

Vanadium is an element with a very rich chemistry that forms an enormous variety of compounds in which the most important oxidation states are +3, +4, and +5.¹ The study

of the element became an intensive field of research in the last decades of the 20th century, after being identified in biological systems² and related with potential therapeutic properties.³

V^{IV} complexes are most commonly observed in the form of compounds of the vanadyl ion, VO^{2+} .⁴ Many complexes are formed by bidentate ligands with a variety of donor

* To whom correspondence should be addressed. E-mail: garribba@uniss.it (E.G.).

sets such as (O, O), (O, N), (O, S), (N, N), (N, S), and (S, S), in which the coordinating atoms belong to different functional groups.^{1,4,5} The most common geometry observed for V^{IV}OL₂ complexes is the square-pyramidal, although distortions toward a trigonal-bipyramidal structure have been reported for some bidentate ligands.^{6,7} For V^{IV}OL₂ species, there is the possibility of cis–trans isomerism, where cis is the bis chelated complex in which the two ligand molecules adopt an (equatorial–equatorial) and an (equatorial–axial) arrangement with respect to the V=O bond and one solvent molecule is coordinated in the fourth equatorial position; trans is the complex in which both ligand molecules adopt an (equatorial–equatorial) arrangement with respect to V=O group.⁵ Non-oxo (so-called “bare”) V^{IV} centers hold important biological functions and have been reported for amavadin⁸ and for the cofactor in vanadium nitrogenase,⁹ but only a few such complexes have been fully characterized in comparison with V^{IV}O species.¹⁰

Several spectroscopic techniques are available for the characterization of V^{IV} species.¹¹ EPR spectroscopy (mainly in conjunction with UV/vis) has revealed itself to be the most powerful tool not only for structurally characterizing V^{IV} complexes^{12,13} but also for identifying the presence of isomers in certain solvents and establishing relationships between the

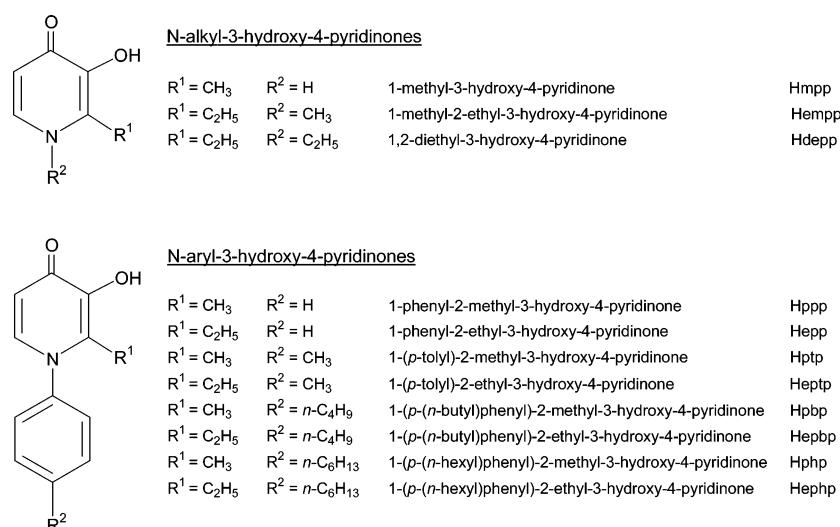
spectroscopic parameters and the degree of distortion toward the two possible geometries for the complexes.^{6,7}

Vanadium plays an important role in life and one of its most relevant properties identified thus far is its capacity to act as an insulin-enhancing agent, either in the form of its inorganic salts or complexed with organic ligands.³ Among the several complexes exhibiting the latter properties, [V^{IV}O(maltolato)₂] (BMOV) has been extensively analyzed from a chemical and pharmacological point of view.^{14,15} Up to this time, many ligands of the 3-hydroxy-4-pyrone type have been studied, mostly by Orvig and his research group;¹⁶ particularly, [V^{IV}O(ethylmaltolato)₂] (BEOV) has completed phase I clinical trials in humans.¹⁷

Replacement of the O atom in the pyrone ring of 3-hydroxy-4-pyrone by a N–R group yields 3-hydroxy-4-pyridinone derivatives.¹⁸ Pyridinone ligands can be obtained by the reaction of pyrones with the appropriate amines and, like pyrones, can act as anionic bidentate ligands with the set (O, O) forming stable complexes, mainly with many trivalent metal ions,¹⁹ such as Fe^{III},²⁰ Al^{III},^{20a,21} Ga^{III},^{21b,21c,21e,22} and In^{III},^{22a,23} but also with divalent ions.²⁴ Pyridinones have

- (1) Crans, D. C.; Smece, J. J.; Gaidamauskas, E.; Yang, L. *Chem. Rev.* **2004**, *104*, 849–902.
- (2) Butler, A.; Walker, J. V. *Chem. Rev.* **1993**, *93*, 1937–1944.
- (3) (a) Shechter, Y.; Karlsh, S. J. D. *Nature* **1980**, *286*, 556–558. (b) Shechter, Y.; Goldwasser, I.; Mironchik, M.; Fridkin, M.; Gefel, D. *Coord. Chem. Rev.* **2003**, *237*, 3–11. (c) Thompson, K. H.; McNeill, J. H.; Orvig, C. *Chem. Rev.* **1999**, *99*, 2561–2571 and references therein. (d) Thompson, K. H.; Orvig, C. *Coord. Chem. Rev.* **2001**, *219–221*, 1033–1053 and references therein.
- (4) Crans, D. C.; Tracey, A. S. In *Vanadium Compounds: Chemistry, Biochemistry, and Therapeutic Applications*; Tracey, A. S.; Crans, D. C., Eds.; ACS Symposium Series 711; American Chemical Society: Washington, DC, 1998; Vol. 31, pp 2–29.
- (5) Garribba, E.; Micera, G.; Lodyga-Chruscinska, E.; Sanna, D. *Eur. J. Inorg. Chem.* **2006**, 2690–2700.
- (6) Cornman, C. R.; Geisre-Bush, K. M.; Rowley, S. R.; Boyle, P. D. *Inorg. Chem.* **1997**, *36*, 6401–6408.
- (7) Garribba, E.; Micera, G.; Panzanelli, A.; Sanna, D. *Inorg. Chem.* **2003**, *42*, 3981–3987.
- (8) (a) Bayer, E.; Koch, E.; Anderegg, G. *Angew. Chem., Int. Ed.* **1987**, *26*, 545–546. (b) Carrondo, M. A. F. de C. T.; Duarte, M. T. L. S.; Costa Pessoa, J.; Silva, J. A. L.; Fraústo da Silva, J. J. R.; Vaz, M. C. T. A.; Vilas-Boas, L. F. J. *Chem. Soc., Chem. Commun.* **1988**, 1158–1159. (c) Carrondo, M. A. F. de C. T.; Duarte, M. T. L. S.; Fraústo da Silva, J. J. R. *Struct. Chem.* **1992**, *3*, 113–119. (d) Smith, P. D.; Berry, R. E.; Harben, S. M.; Beddoes, R. L.; Helliwell, M.; Collison, D.; Garner, C. D. *J. Chem. Soc., Dalton Trans.* **1997**, 4509–4516. (e) Berry, R. E.; Armstrong, E. M.; Beddoes, R. L.; Collison, D.; Ertok, S. N.; Helliwell, M.; Garner, C. D. *Angew. Chem., Int. Ed.* **1999**, *38*, 795–797.
- (9) (a) Robson, R. L.; Eady, R. R.; Richardson, T. J.; Miller, R. W.; Hawkins, M.; Postgate, J. R. *Nature* **1986**, *322*, 388–390. (b) Eady, R. R. In *Metal Ions in Biological Systems*; Sigel, A.; Sigel, H., Eds.; Marcel Dekker: New York, 1995; Vol. 31, pp 363–405 and references therein.
- (10) Morgenstern, B.; Steinhauser, S.; Hegetschweiler, K.; Garribba, E.; Micera, G.; Sanna, D.; Nagy, L. *Inorg. Chem.* **2004**, *43*, 3116–3126 and references therein.
- (11) (a) Garner, C. D.; Collison, D.; Mabbs, F. E. In *Metal Ions in Biological Systems*; Sigel, A.; Sigel, H., Eds.; Marcel Dekker: New York, 1995; pp 617–670. (b) Micera, G.; Sanna, D. In *Vanadium in the Environment Part 1: Chemistry and Biochemistry*; Nriagu, J. O. Ed.; Wiley: New York, 1998; pp 131–166.
- (12) Smith, T. S., II; LoBrutto, R.; Pecoraro, V. L. *Coord. Chem. Rev.* **2002**, *228*, 1–18.
- (13) Mabbs, F. A. *Chem. Soc. Rev.* **1993**, 313–324.
- (14) (a) Caravan, P.; Gelmini, L.; Glover, N.; Herring, F. G.; McNeill, J. H.; Rettig, S. J.; Setyawati, I. A.; Shutter, E.; Sun, Y.; Tracey, A. S.; Yuen, V. G.; Orvig, C. *J. Am. Chem. Soc.* **1995**, *117*, 12759–12770. (b) Sun, Y.; James, B. R.; Rettig, S. J.; Orvig, C. *Inorg. Chem.* **1996**, *35*, 1667–1673. (c) Hanson, G. R.; Sun, Y.; Orvig, C. *Inorg. Chem.* **1996**, *35*, 6507–6512.
- (15) (a) McNeill, J. H.; Yuen, V. G.; Hoveyda, H. R.; Orvig, C. *J. Med. Chem.* **1992**, *35*, 1489–1491. (b) Setyawati, I. A.; Thompson, K. H.; Yuen, V. G.; Sun, Y.; Battell, M.; Lyster, D. M.; Vo, C.; Ruth, T. J.; Zeisler, S.; McNeill, J. H.; Orvig, C. *J. Appl. Physiol.* **1998**, *84*, 569–575.
- (16) (a) Yuen, V. G.; Caravan, P.; Gelmini, L.; Glover, N.; McNeill, J. H.; Setyawati, I. A.; Zhou, Y.; Orvig, C. *J. Inorg. Biochem.* **1997**, *68*, 109–116. (b) Song, B.; Saatchi, K.; Rawji, G. H.; Orvig, C. *Inorg. Chim. Acta* **2002**, *339*, 393–399. (c) Monga, V.; Thompson, K. H.; Yuen, V. G.; Sharma, V.; Patrick, B. O.; McNeill, J. H.; Orvig, C. *Inorg. Chem.* **2005**, *44*, 2678–2688. (d) Saatchi, K.; Thompson, K. H.; Patrick, B. O.; Pink, M.; Yuen, V. G.; McNeill, J. H.; Orvig, C. *Inorg. Chem.* **2005**, *44*, 2689–2697.
- (17) Thompson, K. H.; Liboiron, B. D.; Sun, Y.; Bellman, K. D. D.; Setyawati, I. A.; Patrick, B. O.; Karunaratne, V.; Rawji, G.; Wheeler, J.; Sutton, K.; Bhanot, S.; Cassidy, C.; McNeill, J. H.; Yuen, V. G.; Orvig, C. *J. Biol. Inorg. Chem.* **2003**, *8*, 66–74.
- (18) Although there are several pyridinone ligands that depend on the position of the keto and hydroxy groups (1-hydroxy-2-pyridinones or 1,2-HP, 2-hydroxy-3-pyridinones or 2,3-HP, for example), in this work the word pyridinones will be used to indicate 3-hydroxy-4-pyridinones (3,4-HP).
- (19) Santos, M. A. *Coord. Chem. Rev.* **2002**, *228*, 187–203 and references therein.
- (20) (a) Tsai, W.-C.; Ling, K.-H. *J. Chin. Biochem. Soc.* **1973**, *2*, 70–86. (b) Scarrow, R. C.; Riley, P. E.; Abu-Dari, K.; White, D. L.; Raymond, K. N. *Inorg. Chem.* **1985**, *24*, 954–967. (c) Clarke, E. T.; Martell, A. E.; Reibenspies, J. *Inorg. Chim. Acta* **1992**, *196*, 177–183. (d) Dobbin, P. S.; Hider, R. C.; Hall, A. D.; Taylor, P. D.; Sarpong, P.; Porter, J. B.; Xiao, G.; van der Helm, D. *J. Med. Chem.* **1993**, *36*, 2448–2458.
- (21) (a) Nelson, W. O.; Rettig, S. J.; Orvig, C. *J. Am. Chem. Soc.* **1987**, *109*, 4121–4123. (b) Nelson, W. O.; Karpishin, T. B.; Rettig, S. J.; Orvig, C. *Inorg. Chem.* **1988**, *27*, 1045–1051. (c) Nelson, W. O.; Rettig, S. J.; Orvig, C. *Inorg. Chem.* **1989**, *28*, 3153–3157. (d) Clevette, D. J.; Nelson, W. O.; Nordin, A.; Orvig, C.; Sjöberg, S. *Inorg. Chem.* **1989**, *28*, 2079–2081. (e) Zhang, Z.; Rettig, S. J.; Orvig, C. *Inorg. Chem.* **1991**, *30*, 509–515. (f) Florence, A. L.; Gauthier, A.; Ward, R. J.; Crichton, R. R. *Neurodegeneration* **1995**, *4*, 449–455.
- (22) (a) Clevette, D. J.; Lyster, D. M.; Nelson, W. O.; Rihela, T.; Webb, G. A.; Orvig, C. *Inorg. Chem.* **1990**, *29*, 667–672. (b) Santos, M. A.; Grazina, R.; Neto, A. Q.; Cantino, G.; Gano, L.; Patrício, L. *J. Inorg. Biochem.* **2000**, *78*, 303–311.
- (23) Matsuba, C. A.; Nelson, W. O.; Rettig, S. J.; Orvig, C. *Inorg. Chem.* **1988**, *27*, 3935–3939.

Scheme 1. Ligands



recently been tested and proposed as promising orally effective chelators for Fe^{III} and Al^{III} removal,²⁵ and the compound 1,2-dimethyl-3-hydroxy-4-pyridinone (Hdmpp or DHP), commercially known as Deferiprone, is currently used in the treatment of β -thalassaemia, a genetic disorder to which an iron-overload is associated.^{25a–25d,25f} From the synthetic point of view, 3-hydroxy-4-pyridinones are much more versatile than 3-hydroxy-4-pyrones, as the modification of the side-chain on the nitrogen atom and of the substituents on the six-membered ring allows for a fine-tuning of the hydrophilic/lipophilic balance, a factor that is crucial for in vivo transport properties.^{21d}

Complexation of $\text{V}^{\text{IV}}\text{O}^{26–28}$ and V^{VO}_2 ions^{29,30} with 1,2-dimethyl-3-hydroxy-4-pyridinone (Hdmpp) was studied in aqueous solution by potentiometric and spectroscopic methods. $\text{V}^{\text{IV}}\text{O}$ readily forms various mono and bis complexes, $[\text{V}^{\text{IV}}\text{OL}]^+$, $[\text{V}^{\text{IV}}\text{OL}_2]$, and $[\text{V}^{\text{IV}}\text{OL}_2\text{H}_{-1}]^-$, with the bis chelated $[\text{V}^{\text{IV}}\text{OL}_2]$ species being predominant in the pH range 4–9.^{26–28} The species of composition $[\text{V}^{\text{IV}}\text{OLH}_{-1}]$, first proposed,^{26,27} was better explained in a later study in terms of an EPR-silent dinuclear species $[(\text{V}^{\text{IV}}\text{O})_2\text{L}_2\text{H}_{-2}]$.²⁸ By means of simultaneous potentiometric and spectrophotometric titrations, Taylor also detected and characterized a minor non-oxo species $[\text{V}^{\text{IV}}\text{L}_3]^+$,²⁶ confirmed by the recent data of Buglyó et al.²⁸ Under aerobic conditions, $[\text{V}^{\text{IV}}\text{O}(\text{dmpp})_2]$ is

slowly oxidized to $[\text{V}^{\text{VO}}_2(\text{dmpp})_2]^-$.^{26,30} Some bis chelated $\text{V}^{\text{IV}}\text{O}$ pyridinonate complexes were characterized in the solid state by spectroscopic techniques (UV/vis, EPR, and EXAFS),³¹ and the geometry of the $[\text{V}^{\text{IV}}\text{OL}_2]$ species was described as being slightly distorted square-pyramidal.

The insulin-enhancing properties of $[\text{V}^{\text{IV}}\text{OL}_2]$ compounds formed by 3-hydroxy-4-pyridinones were recently tested in vitro by Rangel et al., who found that they are effective in terms of free fatty acid release from isolated rat adipocytes and have a significantly better insulin-mimetic activity than VOSO_4 .³² A study on the interaction of $[\text{V}^{\text{IV}}\text{O}(\text{dmpp})_2]$ with low-molecular-mass binders present in extra- or intracellular biofluids revealed that, unlike the systems with $[\text{V}^{\text{IV}}\text{O}(\text{maltolato})_2]$, $[\text{V}^{\text{IV}}\text{O}(\text{picolinato})_2(\text{H}_2\text{O})]$, and $[\text{V}^{\text{IV}}\text{O}(\text{6-methylpicolinato})_2]$,³³ the transformation of binary into ternary complexes is almost negligible, also in the presence of a strong ligand as citrate.²⁸ Only serum transferrin can efficiently compete with Hdmpp for $\text{V}^{\text{IV}}\text{O}$ binding.

In the present work, we investigated, through the combined application of spectroscopic (EPR and UV/vis) and potentiometric techniques, the formation of $\text{V}^{\text{IV}}\text{O}$ complexes with 11 pyridinone derivatives (Scheme 1). For the ligands adequately soluble in water (Hmpp, Hempp, Hdepp), potentiometric titrations were performed and the speciation diagrams as a function of pH were established. To the best of our knowledge, no data have been reported in the literature on these systems in aqueous solution. Four new solid derivatives, $[\text{V}^{\text{IV}}\text{O}(\text{depp})_2]$, $[\text{V}^{\text{IV}}\text{O}(\text{eptp})_2]$, $[\text{V}^{\text{IV}}\text{O}(\text{epbp})_2]$, and $[\text{V}^{\text{IV}}\text{O}(\text{ephp})_2]$, were isolated and characterized. The $\text{V}^{\text{IV}}\text{O}$ 3-hydroxy-4-pyridinonate complexes previously described by one of us³¹ have been reexamined in a more exhaustive spectroscopic study and the results obtained are compared with those described for Hdmpp.^{26–28}

(24) Clarke, E. T.; Martell, A. E. *Inorg. Chim. Acta* **1992**, *191*, 57–63.

(25) (a) Kontoghiorghes, G. J. *Lancet* **1985**, *1*, 817–818. (b) Kontoghiorghes, G. J.; Aldouri, M. A.; Hoffbrand, A. V.; Barr, J.; Wonke, B.; Kourouclaris, T.; Sheppard, L. *Br. Med. J.* **1987**, *295*, 1509–1512. (c) Kontoghiorghes, G. J. *Br. Med. J.* **1988**, *296*, 1672–1673. (d) Olivieri, N. F.; Koren, G.; Hermann, C.; Bentur, Y.; Chung, D.; Klein, J.; St Louis, P.; Freedman, M. H.; McClelland, R. A.; Templeton, D. M. *Lancet* **1990**, *336*, 1275–1279. (e) Orvig, C. In *Coordination Chemistry of Aluminium*; Robinson, G., Ed.; VCH Publishers: New York, 1993; pp 85–120. (f) Liu, Z. D.; Hider, R. C. *Coord. Chem. Rev.* **2002**, *232*, 151–171.

(26) Taylor, P. D. *J. Chem. Soc., Chem. Commun.* **1996**, 405–406.

(27) Rangel, M. *Transition Met. Chem.* **2001**, *26*, 219–223.

(28) Buglyó, P.; Kiss, E.; Kiss, T.; Sanna, D.; Garribba, E.; Micera, G. J. *Chem. Soc., Dalton Trans.* **2002**, 2275–2282.

(29) Castro, M. M. C. A.; Geraldes, C. F. G. C.; de Castro, B.; Rangel, M. J. *Inorg. Biochem.* **2000**, *80*, 177–179.

(30) Castro, M. M. C. A.; Aveicilla, F.; Geraldes, C. F. G. C.; de Castro, B.; Rangel, M. *Inorg. Chim. Acta* **2003**, *356*, 142–154.

(31) Burgess, J.; De Castro, B.; Oliveira, C.; Rangel, M.; Schlindwein, W. *Polyhedron* **1997**, *16*, 789–794.

(32) Rangel, M.; Tamura, A.; Fukushima, C.; Sakurai, H. *J. Biol. Inorg. Chem.* **2001**, *6*, 128–132.

(33) Kiss, T.; Kiss, E.; Garribba, E.; Sakurai, H. *J. Inorg. Biochem.* **2000**, *80*, 65–73.

Experimental Section

Chemicals. The ligands were prepared according to procedures described for 3-hydroxy-4-pyridinones.^{21e,34,35} All the other chemicals were Aldrich products of puriss. quality. Their purity and their concentration in solution were determined by the Gran method.³⁶ V^{IV}O solutions were prepared with VOSO₄·5H₂O by following the procedure described in the literature.³⁷ All operations were performed under a purified argon atmosphere in order to avoid oxidation of the V^{IV}O ion.

Potentiometric Measurements. The deprotonation constants of the ligands (pK_a) and the stability constants of V^{IV}O complexes ($\log \beta$) were determined by pH–potentiometric titrations of 2.0 mL samples. The ligand:metal molar ratio was in the range 1:1–10:1, and the concentration of V^{IV}O was 0.001 M. Measurements were carried out at 25 ± 0.1 °C and at a constant ionic strength of 0.1 M KNO₃ with a MOLSPIN pH meter equipped with a digitally operated syringe (the Molspin DSI 0.250 mL) controlled by computer. The titrations were performed with a carbonate-free NaOH solution of known concentration (ca. 0.1 M) using a Russel CMAWL/S7 semi-micro combined electrode, calibrated for hydrogen ion concentration by the method of Irving et al.³⁸ The number of experimental points was 100–150 for each titration curve. The reproducibility of the titration points included in the evaluation was within 0.005 pH units in the whole pH range examined (2–12). The stability constants of the complexes, reported as the logarithm of the overall formation constants $\beta_{pqr} = [\text{VO}_p\text{L}_q\text{H}_r]/[\text{VO}]^p[\text{L}]^q[\text{H}]^r$, where VO is the vanadyl ion, L is the deprotonated form of the ligand, and H is the proton, were calculated with the aid of the SUPERQUAD program.³⁹ The conventional notation has been used, and negative indices for H in the formulas indicate the presence of hydroxo ligands. The following hydroxo species of V^{IV}O were taken into account in the calculations: [V^{IV}O(OH)]⁺ ($\log \beta_{10-1} = -5.94$) and [(V^{IV}O)₂(OH)₂]²⁺ ($\log \beta_{20-2} = -6.95$), with stability constants calculated from the data of Henry et al.⁴⁰ and corrected for the different ionic strengths by use of the Davies equation,⁴¹ [V^{IV}O(OH)₃][–] ($\log \beta_{10-3} = -18.0$) and [(V^{IV}O)₂(OH)₅][–] ($\log \beta_{20-5} = -22.0$).⁴² The uncertainties (σ values) of the stability constants are given in parentheses in Table 1.

Preparation of [V^{IV}OL₂] Complexes. [V^{IV}OL₂] complexes were prepared by dissolving stoichiometric amounts of VOSO₄·5H₂O and the ligand in water, adjusting the pH to 9 with a diluted solution of NaOH, and refluxing for about 1 h. The solids formed were filtered when the solution was still warm and dried in vacuo over P₂O₅. [V^{IV}O(depp)₂]. Anal. Calcd for C₁₈H₂₄N₂O₅V (399.34): C, 54.14; H, 6.06; N, 7.01; H₂O, 0.0; V₂O₅, 22.8. Found: C, 54.35; H, 5.97; N, 7.27; H₂O, 0.0; V₂O₅, 23.2. [V^{IV}O(eptp)₂]. Anal. Calcd for C₂₈H₂₈N₂O₅V (523.48): C, 64.24; H, 5.39; N, 5.35; H₂O, 0.0;

Table 1. pK_a of the Ligands and Stability Constants of the V^{IV}O Complexes ($\log \beta$) at 25.0 ± 0.1 °C and $I = 0.1$ M (KNO₃)^a

ligand/complex	$pK_a/\log \beta$		
	Hmpp	Hempp	Hdepp
–OH/–N _{pyr} H ⁺ (pK_{a1})	3.50(2)	3.69(2)	3.78(1)
–OH (pK_{a2})	9.70(1)	9.85(1)	9.92(1)
VOL	12.05(1)	12.20(1)	12.30(1)
VOL ₂	22.42(2)	22.90(1)	23.10(2)
VOL ₂ H _{–1}	11.95(2)	12.25(2)	12.35(1)
(VO) ₂ L ₂ H _{–2}	17.91(12)	19.51(16)	20.00(15)
VL ₃ ⁺ ·H ₂ O	37.95(1)	38.70(3)	39.10(1)

^a The uncertainties (σ values) of the stability constants are given in parentheses.

V₂O₅, 17.4. Found: C, 64.36; H, 5.35; N, 5.21; H₂O, 0.0; V₂O₅, 17.5. [V^{IV}O(epbp)₂]. Anal. Calcd for C₃₄H₄₀N₂O₅V (607.64): C, 67.21; H, 6.63; N, 4.61; H₂O, 0.0; V₂O₅, 15.0. Found: C, 67.03; H, 6.78; N, 4.44; H₂O, 0.0; V₂O₅, 14.6. [V^{IV}O(eph)₂]. Anal. Calcd for C₃₈H₄₈N₂O₅V (663.75): C, 68.76; H, 7.29; N, 4.22; H₂O, 0.0; V₂O₅, 13.7. Found: C, 68.87; H, 7.10; N, 4.06; H₂O, 0.0; V₂O₅, 14.0.

Preparation of [V^{IV}L₃]⁺ Complexes. [V^{IV}OL₂] complex (10 μ M) was dissolved in 1 mL of concentrated CH₃COOH. To the solution was added 50 μ M of ligand HL. The formation of the [V^{IV}L₃]⁺ complex can be detected through UV/vis and EPR spectroscopies. EPR spectra were recorded on a 0.01 M solution of [V^{IV}L₃]⁺ and electronic absorption spectra by diluting the sample to 0.25 mM. In particular, the absence of EPR signals in the ranges 2700–2800 and 3900–4000 G, which are assigned to V^{IV}O species, must be verified.

Spectroscopic and Analytical Measurements. Anisotropic EPR spectra were recorded on aqueous solutions with an X-band (9.15 GHz) Varian E-9 spectrometer in the temperature range 120–140 K. The spectra were simulated with the computer suite program Bruker WinEPR/SimFonia. Electronic spectra were obtained with a Perkin–Elmer Lambda 9 spectrometer and deconvoluted with Origin. Elemental analyses (C, H, N) were performed with a Perkin–Elmer 240 B analyzer. The thermogravimetric studies, which allowed the determination of the V₂O₅ and H₂O contents, were carried out with a Perkin–Elmer TGS-2 instrument under a nitrogen atmosphere.

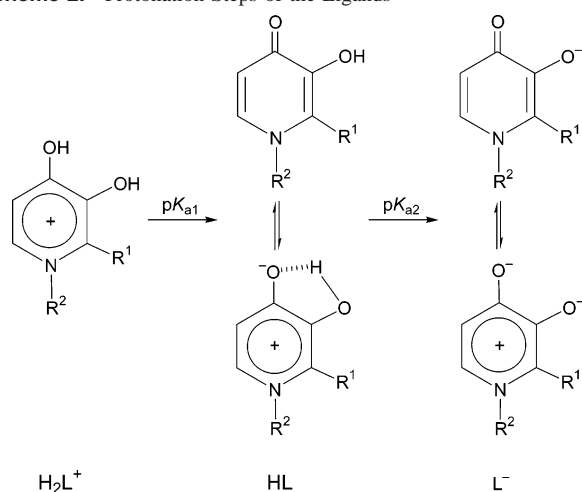
Results

Determination of Acid–Base Properties of Ligands.

Potentiometric titrations were performed on the alkyl ligands Hmpp, Hempp, and Hdepp, the only three ligands adequately soluble in water. From the fully protonated ligands, two stepwise deprotonation processes are observed in the pH range that we are able to titrate. The values obtained for the two acidity constants, designated as $pK_{a1}(\text{H}_2\text{L}^+)$ and $pK_{a2}(\text{HL})$, are presented in Table 1, and the protonation equilibria considered are shown in Scheme 2. When the differences in the experimental conditions are taken into consideration, the two pK_a values determined for Hmpp, Hempp, and Hdepp are in good agreement with published data.^{20d,21d,22a,22b,24,28}

The values of the first pK_a lie in the range 3.5–3.8 and are in accord with the results previously reported.^{20d,21d,22a,22b,24,28} There is a common agreement in the literature that the protonation of HL species takes place mainly on the carbonyl-O rather than on the nitrogen-N of the ring. This

- (34) Färber, M.; Osiander, H.; Severin, T. *J. Heterocycl. Chem.* **1994**, *31*, 947–956.
 (35) Finnegan, M. M.; Rettig, S. J.; Orvig, C. *J. Am. Chem. Soc.* **1986**, *108*, 5033–5035.
 (36) Gran, G. *Acta Chem. Scand.* **1950**, *4*, 559–577.
 (37) Nagypál, I.; Fábán, I. *Inorg. Chim. Acta* **1982**, *61*, 109–113.
 (38) Irving, H.; Miles, M. G.; Pettit, L. D. *Anal. Chim. Acta* **1967**, *38*, 475–481.
 (39) Gans, P.; Vacca, A.; Sabatini, A. *J. Chem. Soc., Dalton Trans.* **1985**, 1195–1200.
 (40) Henry, R. P.; Mitchell, P. C. H.; Prue, J. E. *J. Chem. Soc., Dalton Trans.* **1973**, 1156–1159.
 (41) Davies, C. W. *J. Chem. Soc.* **1938**, 2093–2098.
 (42) (a) Komura, A.; Hayashi, M.; Imanaga, H. *Bull. Chem. Soc. Jpn.* **1977**, *50*, 2927–2931. (b) Vilas Boas, L. F.; Costa Pessoa, J. In *Comprehensive Coordination Chemistry*; Wilkinson, G., Gillard, R. D., McCleverty, J. A., Eds.; Pergamon Press: Oxford, U.K., 1987; Vol. 3, pp 453–583.

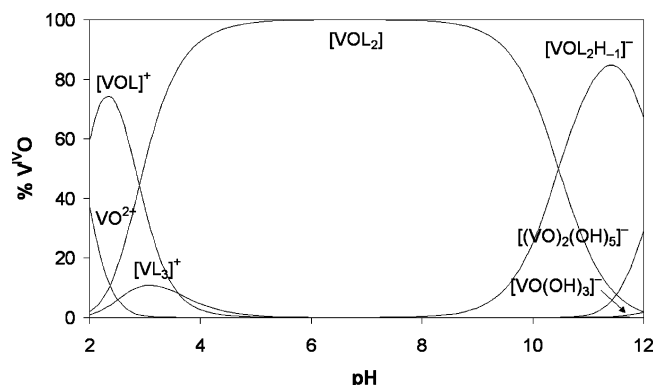
Scheme 2. Protonation Steps of the Ligands

was recently confirmed by a very slight change in the chemical shifts of the methyl protons on the nitrogen atom of Hdmp. The $\text{p}K_{\text{a}1}$ values obtained for the 3-hydroxy-4-pyridinones are about 5 orders of magnitude higher than those reported for 3-hydroxy-4-pyrones,⁴³ and can be explained taking into account that in pyridinones the oxygen in the heterocyclic ring is replaced by a nitrogen atom, which is more efficient in delocalizing the positive charge in the ring and favors the stabilization of the 3,4-dihydroxypyridinium cation H_2L^+ , a highly delocalized pseudo-aromatic π electronic system (Scheme 2).

The values of $\text{p}K_{\text{a}2}$ are in the range 9.7–9.9 (Table 1); a comparison with those reported for two 3-hydroxy-4-pyrones such as kojic acid (7.67) and maltol (8.44)⁴⁴ shows that pyridinones are stronger bases. The values for pyridinones are related to the partially negatively charged oxygen in position 4 of the ring, which confirms the contribution of the zwitterionic form in the neutral form HL; this is due to the transfer of the nitrogen lone pair to the carbonyl oxygen in position 4 of the ring, which is promoted by the re-establishment of the pseudo-aromatic character (Scheme 2).

The presence of different substituents in positions 1 and 2 of the pyridinone ring is reflected by the values of $\text{p}K_{\text{a}}$ listed in Table 1, which indicate that the basicity of the ligands increases in the order hydrogen < methyl < ethyl. This is due to the electron-releasing properties of the alkyl groups. However, the effect is smaller than 0.3 $\text{p}K_{\text{a}}$ units and so does not affect the predominance of the neutral species in a wide pH range, including physiological pH.

Characterization of Metal–Ligand Species in Aqueous Solution. The potentiometric titrations performed in aqueous solution suggest that a 1:2 metal:ligand molar ratio is enough to prevent hydrolytic processes. The equilibrium constants are shown in Table 1 and are consistent with a model that assumes the $[\text{V}^{\text{IV}}\text{OL}]^+$, $[\text{V}^{\text{IV}}\text{OL}_2]$, $[\text{V}^{\text{IV}}\text{OL}_2\text{H}_{-1}]^-$, $[(\text{V}^{\text{IV}}\text{O})_2\text{L}_2\text{H}_{-2}]$, and $[\text{V}^{\text{IV}}\text{L}_3]^+$ species. The order of stability of all the complexes is Hdepp > Hempp > Hmpp and

**Figure 1.** Species distribution for the $\text{V}^{\text{IV}}\text{O}/\text{Hmpp}$ system with a 1:3 metal:ligand molar ratio and a $\text{V}^{\text{IV}}\text{O}$ concentration of 1 mM.**Table 2.** EPR Parameters and Donor Sets for the $\text{V}^{\text{IV}}\text{O}$ Complexes in Aqueous Solution

ligand	complex	g_z	A_z^a	donor set
Hmpp	VOL	1.939	170	$[(\text{O}^-, \text{O}^-); \text{H}_2\text{O}; \text{H}_2\text{O}; \text{H}_2\text{O}^{\text{ax}}]$
	cis-VOL ₂	1.941	166	$[(\text{O}^-, \text{O}^-); (\text{O}^-, \text{O}^{\text{ax}}); \text{H}_2\text{O}]$
	trans-VOL ₂	1.950	158	$[(\text{O}^-, \text{O}^-); (\text{O}^-, \text{O}^-)]$
	cis-VOL ₂ H ₋₁	1.943	162	$[(\text{O}^-, \text{O}^-); (\text{O}^-, \text{O}^{\text{ax}}); \text{OH}^-]$
Hempp	VOL	1.939	170	$[(\text{O}^-, \text{O}^-); \text{H}_2\text{O}; \text{H}_2\text{O}; \text{H}_2\text{O}^{\text{ax}}]$
	cis-VOL ₂	1.941	166	$[(\text{O}^-, \text{O}^-); (\text{O}^-, \text{O}^{\text{ax}}); \text{H}_2\text{O}]$
	trans-VOL ₂	1.950	158	$[(\text{O}^-, \text{O}^-); (\text{O}^-, \text{O}^-)]$
	cis-VOL ₂ H ₋₁	1.943	162	$[(\text{O}^-, \text{O}^-); (\text{O}^-, \text{O}^{\text{ax}}); \text{OH}^-]$
Hdepp	VOL	1.939	170	$[(\text{O}^-, \text{O}^-); \text{H}_2\text{O}; \text{H}_2\text{O}; \text{H}_2\text{O}^{\text{ax}}]$
	cis-VOL ₂	1.941	166	$[(\text{O}^-, \text{O}^-); (\text{O}^-, \text{O}^{\text{ax}}); \text{H}_2\text{O}]$
	trans-VOL ₂	1.951	158	$[(\text{O}^-, \text{O}^-); (\text{O}^-, \text{O}^-)]$
	cis-VOL ₂ H ₋₁	1.944	161	$[(\text{O}^-, \text{O}^-); (\text{O}^-, \text{O}^{\text{ax}}); \text{OH}^-]$
Hppp	VOL	1.938	171	$[(\text{O}^-, \text{O}^-); \text{H}_2\text{O}; \text{H}_2\text{O}; \text{H}_2\text{O}^{\text{ax}}]$
	cis-VOL ₂	1.940	167	$[(\text{O}^-, \text{O}^-); (\text{O}^-, \text{O}^{\text{ax}}); \text{H}_2\text{O}]$
	trans-VOL ₂	1.950	159	$[(\text{O}^-, \text{O}^-); (\text{O}^-, \text{O}^-)]$
	cis-VOL ₂ H ₋₁	1.943	162	$[(\text{O}^-, \text{O}^-); (\text{O}^-, \text{O}^{\text{ax}}); \text{OH}^-]$
Hepp	VOL	1.939	170	$[(\text{O}^-, \text{O}^-); \text{H}_2\text{O}; \text{H}_2\text{O}; \text{H}_2\text{O}^{\text{ax}}]$
	cis-VOL ₂	1.941	166	$[(\text{O}^-, \text{O}^-); (\text{O}^-, \text{O}^{\text{ax}}); \text{H}_2\text{O}]$
	trans-VOL ₂	1.950	159	$[(\text{O}^-, \text{O}^-); (\text{O}^-, \text{O}^-)]$
	cis-VOL ₂ H ₋₁	1.943	162	$[(\text{O}^-, \text{O}^-); (\text{O}^-, \text{O}^{\text{ax}}); \text{OH}^-]$
Hptp	VOL	1.939	171	$[(\text{O}^-, \text{O}^-); \text{H}_2\text{O}; \text{H}_2\text{O}; \text{H}_2\text{O}^{\text{ax}}]$
	cis-VOL ₂	1.940	166	$[(\text{O}^-, \text{O}^-); (\text{O}^-, \text{O}^{\text{ax}}); \text{H}_2\text{O}]$
	trans-VOL ₂	1.950	158	$[(\text{O}^-, \text{O}^-); (\text{O}^-, \text{O}^-)]$
	cis-VOL ₂ H ₋₁	1.943	162	$[(\text{O}^-, \text{O}^-); (\text{O}^-, \text{O}^{\text{ax}}); \text{OH}^-]$
Heptp	VOL	1.938	170	$[(\text{O}^-, \text{O}^-); \text{H}_2\text{O}; \text{H}_2\text{O}; \text{H}_2\text{O}^{\text{ax}}]$
	cis-VOL ₂	1.941	167	$[(\text{O}^-, \text{O}^-); (\text{O}^-, \text{O}^{\text{ax}}); \text{H}_2\text{O}]$
	trans-VOL ₂	1.951	158	$[(\text{O}^-, \text{O}^-); (\text{O}^-, \text{O}^-)]$
	cis-VOL ₂ H ₋₁	1.944	161	$[(\text{O}^-, \text{O}^-); (\text{O}^-, \text{O}^{\text{ax}}); \text{OH}^-]$
Hpbb	VOL	1.938	171	$[(\text{O}^-, \text{O}^-); \text{H}_2\text{O}; \text{H}_2\text{O}; \text{H}_2\text{O}^{\text{ax}}]$
	cis-VOL ₂	1.941	166	$[(\text{O}^-, \text{O}^-); (\text{O}^-, \text{O}^{\text{ax}}); \text{H}_2\text{O}]$
	trans-VOL ₂	1.950	158	$[(\text{O}^-, \text{O}^-); (\text{O}^-, \text{O}^-)]$
	cis-VOL ₂ H ₋₁	1.943	162	$[(\text{O}^-, \text{O}^-); (\text{O}^-, \text{O}^{\text{ax}}); \text{OH}^-]$
Hepbp	VOL	1.939	170	$[(\text{O}^-, \text{O}^-); \text{H}_2\text{O}; \text{H}_2\text{O}; \text{H}_2\text{O}^{\text{ax}}]$
	cis-VOL ₂	1.941	167	$[(\text{O}^-, \text{O}^-); (\text{O}^-, \text{O}^{\text{ax}}); \text{H}_2\text{O}]$
	trans-VOL ₂	1.950	158	$[(\text{O}^-, \text{O}^-); (\text{O}^-, \text{O}^-)]$
	cis-VOL ₂ H ₋₁	1.943	162	$[(\text{O}^-, \text{O}^-); (\text{O}^-, \text{O}^{\text{ax}}); \text{OH}^-]$
Hphp	VOL	1.938	171	$[(\text{O}^-, \text{O}^-); \text{H}_2\text{O}; \text{H}_2\text{O}; \text{H}_2\text{O}^{\text{ax}}]$
	cis-VOL ₂	1.940	167	$[(\text{O}^-, \text{O}^-); (\text{O}^-, \text{O}^{\text{ax}}); \text{H}_2\text{O}]$
	trans-VOL ₂	1.950	159	$[(\text{O}^-, \text{O}^-); (\text{O}^-, \text{O}^-)]$
	cis-VOL ₂ H ₋₁	1.943	162	$[(\text{O}^-, \text{O}^-); (\text{O}^-, \text{O}^{\text{ax}}); \text{OH}^-]$
Hephp	VOL	1.939	170	$[(\text{O}^-, \text{O}^-); \text{H}_2\text{O}; \text{H}_2\text{O}; \text{H}_2\text{O}^{\text{ax}}]$
	cis-VOL ₂	1.941	166	$[(\text{O}^-, \text{O}^-); (\text{O}^-, \text{O}^{\text{ax}}); \text{H}_2\text{O}]$
	trans-VOL ₂	1.950	158	$[(\text{O}^-, \text{O}^-); (\text{O}^-, \text{O}^-)]$
	cis-VOL ₂ H ₋₁	1.944	161	$[(\text{O}^-, \text{O}^-); (\text{O}^-, \text{O}^{\text{ax}}); \text{OH}^-]$

^a A_z measured in units of $1 \times 10^{-4} \text{ cm}^{-1}$.

reflects the basicity of the ligands. The distribution diagram for the binary system formed by $\text{V}^{\text{IV}}\text{O}$ and Hmpp is shown in Figure 1.

The EPR data presented in Table 2 corroborate the proposed set of equilibria and, as an example, the spectra

(43) Choux, G.; Benoit, R. L. *J. Org. Chem.* **1967**, *32*, 3974–3977.

(44) Buglyó, P.; Kiss, E.; Fábrián, I.; Kiss, T.; Sanna, D.; Garribba, E.; Micera, G. *Inorg. Chim. Acta* **2000**, *306*, 174–183.

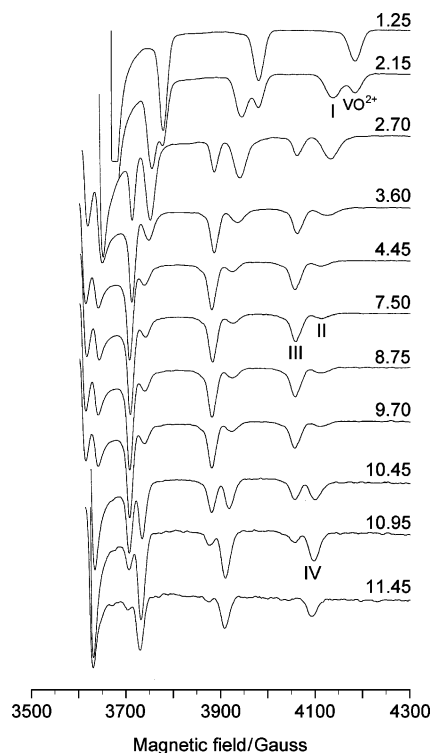


Figure 2. High-field region of the X-band anisotropic EPR spectra recorded at 140 K as a function of pH on an aqueous solution of V^{IV}O and Hempp with a 1:2 metal:ligand molar ratio and a V^{IV}O concentration of 4 mM. **I**, **II**, **III**, and **IV** denote the [V^{IV}OL]⁺, *cis*-[V^{IV}OL₂], *trans*-[V^{IV}OL₂], and *cis*-[V^{IV}OL₂H₋₁]⁻ complexes, respectively.

recorded for Hempp are displayed in Figure 2. At L:M = 2, the complexation starts at pH < 2 with the formation of the [V^{IV}OL]⁺ complex (**I** in Figure 2), characterized by g_z in the range 1.938–1.939 and A_z in the range $170\text{--}171 \times 10^{-4} \text{ cm}^{-1}$ (Table 2). A_z values, calculated with the additivity rule, support an equatorial (O⁻, O⁻) coordination of the ligands.⁴⁵

A significant improvement in the analysis of the data is achieved by considering a dinuclear species with a [(V^{IV}O)₂L₂H₋₂] stoichiometry, mainly observed in equimolar solution. The formation of such a species can be rationalized in terms of the deprotonation of an equatorially coordinated water molecule in [V^{IV}OL]⁺ and the dimerization of the resulting [V^{IV}OL(OH)] unit according to the rule proposed by Felcman and Fraústo da Silva for the hydrolysis of V^{IV}O species.⁴⁶ Its presence is confirmed by a significant loss in intensity of the EPR signal in equimolar solution around pH 5.0, followed by the formation of a precipitate.

At L:M = 2 or at higher ligand excess, the bis complexes [V^{IV}OL₂] are the predominant species between pH 4 and 10. In this pH range, the EPR spectra indicate a major ($g_z = 1.950\text{--}1.951$ and $A_z = 158\text{--}159 \times 10^{-4} \text{ cm}^{-1}$, **III** in Figure 2) and a minor species ($g_z = 1.940\text{--}1.941$ and $A_z = 166\text{--}167 \times 10^{-4} \text{ cm}^{-1}$, **II** in Figure 2). For each system, the ratio between the intensities of the two signals remains unchanged as a function of pH and, depending on the ligand, ranges

from 80:20 to 90:10. These results are in agreement with those previously reported²⁸ and can be explained in terms of a *cis*–*trans* equilibrium observed for several V^{IV}O systems, like those with malonate and oxalate,⁴⁴ 6-methylpicolinate,⁴⁷ and 8-hydroxyquinolate.⁴⁸ A comparison between the experimental and calculated EPR parameters suggests that the major species is the *trans* isomer, with the four oxygen donors of the two ligand molecules occupying the equatorial sites of V^{IV}O ion. The spectral parameters are comparable with those of the bis chelated species of catechol and 3,4-dihydroxybenzoic acid,⁴⁹ meaning that pyridinones coordinate the V^{IV}O ion with a donor set similar to that (O⁻, O⁻) observed for catechols, rather than that (CO, O⁻) of maltol.^{14a,14c,44} The weaker resonances in the pH range 4–10 are assigned to the *cis* isomer of the [V^{IV}OL₂] complex, in which a water molecule in *cis* position with respect to the V=O bond is coordinated in the equatorial plane and one of the two ligand molecules adopts an (equatorial–axial) coordination mode.

The deprotonation of the equatorial water in [V^{IV}OL₂] yields a [V^{IV}OL₂H₋₁]⁻ species (**IV** in Figure 2), with a hydroxo ion in *cis* to the V=O group. The conversion from *cis*-[V^{IV}OL₂(H₂O)] to *cis*-[V^{IV}OL₂(OH)]⁻ species is indicated in the EPR spectra by the change of the g_z and A_z values. Particularly, the parameters for *cis*-[V^{IV}OL₂H₋₁]⁻ ($g_z = 1.943\text{--}1.944$ and $A_z = 161\text{--}162 \times 10^{-4} \text{ cm}^{-1}$, Table 2) are those expected for a species with three deprotonated oxygen donors and a OH⁻ on the equatorial plane of the V^{IV}O ion. On the basis of the additivity rule, the replacement of a H₂O by a OH⁻ donor should decrease A_z by $\sim(5\text{--}6) \times 10^{-4} \text{ cm}^{-1}$.⁴⁵ As for Hdmpp,²⁸ the pK values for the deprotonation of the equatorially coordinated water molecule are rather high, in the range 10.47–10.75, confirming that pyridinones are stronger donors than kojate or maltolate.⁴⁴

For all the systems, we observed an intense deep violet color in the acidic pH range 2–4, suggesting the formation of a tris chelated non-oxo V^{IV} complex with $3 \times (\text{O}^-, \text{O}^-)$ donor set, as previously reported for catechol and its derivatives,⁵⁰ as well as for Hdmpp.^{26,28} The formation of these non-oxo species, not observed with pyrone ligands, reflects the stronger basic properties of pyridinones.

Synthesis and Characterization of Non-Oxo [V^{IV}L₃]⁺ Complexes. In aqueous solutions containing V^{IV}O and ligands at molar ratios as high as 1:100, EPR spectroscopy indicates the formation of [V^{IV}L₃]⁺ species, which always coexist with [V^{IV}OL]⁺ and [V^{IV}OL₂]. Synthesis of the tris chelated species may be achieved by dissolving the solid [V^{IV}OL₂] in concentrated acetic acid containing an excess of ligand. The acidic media induces the cleavage of the V=O

(45) Chasteen N. D. In *Biological Magnetic Resonance*; Berliner, L. J.; J. Reuben, J. Eds.; Plenum Press: New York, 1981; Vol. 3, pp 53–119.

(46) Felcman, J.; Fraústo da Silva, J. J. R. *Talanta* **1983**, *30*, 565–570.

(47) Kiss, E.; Garribba, E.; Micera, G.; Kiss, T.; Sakurai, H. *J. Inorg. Biochem.* **2000**, *78*, 97–108.

(48) Garribba, E.; Micera, G.; Sanna, D.; Chruscinska, E. *Inorg. Chim. Acta* **2003**, *348*, 97–106.

(49) Jezowska-Bojczuk, M.; Koslowski, H.; Zubor, A.; Kiss, T.; Branca, M.; Micera, G.; Dessì, A. *J. Chem. Soc., Dalton Trans.* **1990**, 2903–2907.

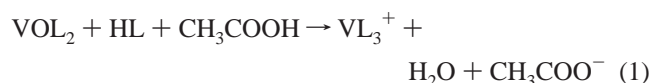
(50) Buglyó, P.; Dessì, A.; Kiss, T.; Micera, G.; Sanna, D. *J. Chem. Soc., Dalton Trans.* **1993**, 2057–2063.

Table 3. EPR and Electronic Absorption Parameters for Tris Chelated Non-Oxo V^{IV} Complexes in CH₃COOH

complex	g_x	g_y	g_z	A_x^a	A_y^a	A_z^a	$ A_x - A_y ^a$	λ (ϵ) ^b
[V(mpp) ₃] ⁺	1.916	1.914	1.988	118.2	101.9	10.2	16.3	348(7600), 445(6700), 528(7900), 596(7300)
[V(empp) ₃] ⁺	1.918	1.916	1.989	122.1	97.8	10.2	24.3	338(7600), 440(6500), 524(8100), 608(7200)
[V(depp) ₃] ⁺	1.918	1.916	1.988	122.0	97.9	10.2	24.1	337(7600), 438(6500), 522(8100), 609(7100)
[V(ppp) ₃] ⁺	1.916	1.913	1.987	118.6	101.7	10.0	16.9	350(7500), 446(6700), 530(7900), 594(7300)
[V(epp) ₃] ⁺	1.918	1.916	1.988	122.4	98.1	10.2	24.3	338(7500), 441(6400), 524(8000), 610(7200)
[V(ftp) ₃] ⁺	1.915	1.914	1.988	117.9	102.0	10.1	15.9	351(7500), 443(6700), 528(8000), 594(7300)
[V(eptp) ₃] ⁺	1.918	1.916	1.988	122.7	98.2	10.0	24.5	339(7600), 439(6500), 523(8100), 611(7200)
[V(pbp) ₃] ⁺	1.916	1.914	1.988	118.1	102.3	10.1	15.8	352(7600), 444(6600), 527(7900), 595(7300)
[V(epbp) ₃] ⁺	1.919	1.916	1.988	122.6	98.5	9.9	24.1	336(7600), 442(6400), 526(8100), 609(7200)
[V(phpp) ₃] ⁺	1.916	1.914	1.988	118.5	102.2	9.8	16.3	349(7600), 444(6700), 529(7900), 592(7300)
[V(ephpp) ₃] ⁺	1.918	1.916	1.988	121.9	98.4	10.3	23.5	340(7600), 440(6500), 525(8100), 612(7200)

^a A_x , A_y , A_z , and $|A_x - A_y|$ measured in units of $1 \times 10^{-4} \text{ cm}^{-1}$. ^b λ measured in nanometers and ϵ in $\text{M}^{-1} \text{ cm}^{-1}$.

bond with the consequent formation of a water molecule⁵¹



The formation of $[\text{V}^{\text{IV}}\text{L}_3]^+$ species can be demonstrated by EPR spectroscopy. All the experimental EPR spectra were simulated, and the parameters are reported in Table 3. The g and A values ($g_z \approx 2 > g_x \approx g_y$ and $A_z \ll A_x \approx A_y$), with A_z close to $10 \times 10^{-4} \text{ cm}^{-1}$, are consistent with an unpaired electron residing in a nondegenerate molecular orbital that is largely d_{z^2} in character.⁵² This electronic configuration suggests for the non-oxo species a distorted geometry intermediate between the octahedron and the trigonal prism,⁵³ as a consequence of the steric requirements of the ligand molecules.⁵⁴ On the basis of the spectral parameters, the non-oxo V^{IV} complexes can be grouped in two sets of compounds: one with ligands with $\text{R}^1 = \text{methyl}$ (Hmpp, Hppp, Htp, Hpbp, Hphp) and the other with ligands with $\text{R}^2 = \text{ethyl}$ (Hempp, Hdepp, Hepp, Heptp, Hepbp, Hephp). The spectra of $[\text{V}^{\text{IV}}(\text{empp})_3]^+$ and $[\text{V}^{\text{IV}}(\text{mpp})_3]^+$ are shown in Figure 3, with the second being very similar to that of Hdmp.²⁸ The anisotropy between the x and y axes, expressed as $|A_x - A_y|$, can be related to the degree of rhombic distortion of the species and depends mainly on the steric hindrance of the substituents on the carbon in the α -position with respect to 3-hydroxy group. Table 3 suggests that the bulkier ethyl ($|A_x - A_y| \approx 24\text{--}25 \times 10^{-4} \text{ cm}^{-1}$) produces a bigger distortion than the methyl group ($|A_x - A_y| \approx 16\text{--}17 \times 10^{-4} \text{ cm}^{-1}$).

The electronic absorption spectra of the non-oxo species were recorded in CH₃COOH, and that of $[\text{V}^{\text{IV}}(\text{empp})_3]^+$ is presented in Figure 4. All the complexes show an intense deep violet color. The detection of four bands between 350 and 750 nm with ϵ in the range 2000–12000 $\text{M}^{-1} \text{ cm}^{-1}$ is a distinctive feature of the non-oxo V^{IV} complexes.⁵⁵ Such

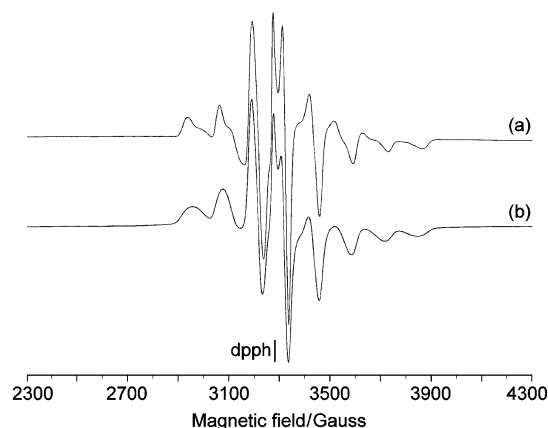


Figure 3. X-band anisotropic EPR spectra recorded at 140 K in CH₃COOH on tris chelated non-oxo V^{IV} species with a V^{IV} concentration of 0.01 M: (a) $[\text{V}^{\text{IV}}(\text{empp})_3]^+$ and (b) $[\text{V}^{\text{IV}}(\text{mpp})_3]^+$. Diphenylpicrylhydrazyl (dpph) is the standard field marker ($g = 2.0036$).

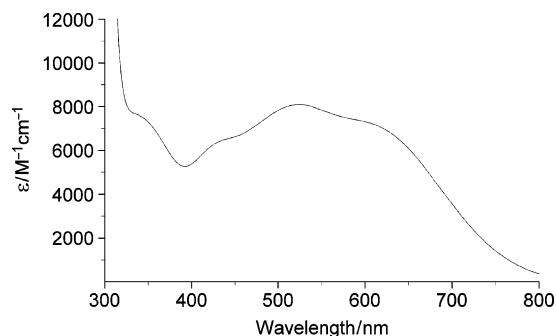


Figure 4. Electronic absorption spectrum recorded in CH₃COOH of the $[\text{V}^{\text{IV}}(\text{empp})_3]^+$ complex with a V^{IV} concentration of 0.25 mM.

bands have been interpreted in terms of charge-transfer transitions, which cover the d–d absorptions.^{55,56} First, the transitions above 500 nm have been assigned to $\text{L}(\pi) \rightarrow \text{V}(\text{d})$ and those below 400 nm to $\text{V}(\text{d}) \rightarrow \text{L}(\pi)$ charge transfers.^{55a,55b,56} Subsequently, Raymond and co-workers proposed that, for non-oxo V^{IV} species formed by catecholates, all the transitions must be considered ligand-to-metal charge

- (51) Dessì, A.; Micera, G.; Sanna, D.; Strinna Erre, L. *J. Inorg. Biochem.* **1992**, *48*, 279–287.
 (52) Desideri, A.; Raynor, J. B.; Diamantis, A. A. *J. Chem. Soc., Dalton Trans.* **1978**, 423–426.
 (53) Olk, R.-M.; Dietzsch, W.; Kirmse, R.; Stach, J.; Hoyer, E.; Golic, L. *Inorg. Chim. Acta* **1987**, *128*, 251–259.
 (54) Branca, M.; Micera, G.; Dessì, A.; Sanna, D.; Raymond, K. N. *Inorg. Chem.* **1990**, *29*, 1586–1589.

- (55) (a) Cooper, S. R.; Koh, Y. B.; Raymond, K. N. *J. Am. Chem. Soc.* **1982**, *104*, 5092–5102. (b) Hawkins, C. J.; Kabanos, T. A. *Inorg. Chem.* **1989**, *28*, 1084–1087. (c) Karpishin, T. B.; Dewey, T. M.; Raymond, K. N. *J. Am. Chem. Soc.* **1993**, *115*, 1842–1851. (d) Klich, P. R.; Daniher, A. T.; Challen, P. R.; McConville, D. B.; Youngs, W. *J. Inorg. Chem.* **1996**, *35*, 347–356.
 (56) (a) VonDeele, R. B.; Fay, R. C. *J. Am. Chem. Soc.* **1972**, *94*, 7935–7936. (b) Hambley, T. W.; Hawkins, C. J.; Kabanos, T. A. *Inorg. Chem.* **1987**, *26*, 3740–3745.

Table 4. EPR Parameters for Bis Chelated Solid V^{IV}O Complexes in DMF

complex	g_x	g_y	g_z	A_x^a	A_y^a	A_z^a	$ A_x - A_y ^a$
[VO(mpp) ₂]	1.985	1.978	1.951	45.4	53.1	158.1	7.7
[VO(empp) ₂]	1.985	1.978	1.951	45.3	53.1	157.8	7.8
[VO(depp) ₂]	1.985	1.978	1.951	45.2	53.2	157.7	8.0
[VO(ppp) ₂]	1.984	1.977	1.950	45.3	53.2	158.1	7.9
[VO(epp) ₂]	1.985	1.978	1.950	45.4	53.5	158.0	8.1
[VO(ftp) ₂]	1.985	1.978	1.950	45.4	53.2	158.2	7.8
[VO(eftp) ₂]	1.985	1.978	1.951	45.1	53.2	158.1	8.1
[VO(pbp) ₂]	1.984	1.978	1.951	45.5	53.2	158.2	7.7
[VO(epbp) ₂]	1.986	1.978	1.951	45.2	53.4	157.9	8.2
[VO(php) ₂]	1.985	1.977	1.950	45.5	53.3	158.3	7.8
[VO(ephp) ₂]	1.985	1.978	1.951	45.3	53.2	157.8	7.9

^a A_x , A_y , A_z , and $|A_x - A_y|$ measured in units of $1 \times 10^{-4} \text{ cm}^{-1}$.

transfers between the a_2 and e_π orbitals of catechol and $e_a(d_{xy}, d_{x^2-y^2})$ and $e_b(d_{xz}, d_{yz})$ orbitals of vanadium in the D_3 symmetry of the complexes;^{55d} particularly, they attributed the four absorptions to the $L(a_2) \rightarrow V(e_a)$, $L(e_\pi) \rightarrow V(e_a)$, $L(a_2) \rightarrow V(e_b)$ and $L(e_\pi) \rightarrow V(e_b)$ transitions, in order of increasing energy.^{55d} An analysis of our data (Table 3) supports, however, two different types of electronic spectra related to the two types of distortion of the species, according to the presence of a methyl or an ethyl on the C atom in the α -position to 3-hydroxy group (Table 3). This suggests, of course, that the energy of the $e_a(d_{xy}, d_{x^2-y^2})$ and $e_b(d_{xz}, d_{yz})$ vanadium orbitals depends on the degree of distortion of the complexes, as confirmed by EPR spectra, even if a more detailed analysis is necessary to clarify this point.

Synthesis and Characterization of [V^{IV}OL₂] Solid Complexes. The reaction of the ligands Hdepp, Heptp, Hepbp, and Hphp (see Scheme 1) with VOSO₄·5H₂O gives rise to the formation of [V^{IV}OL₂] solid complexes. The composition has been determined through the combined application of elemental (C, H, N) and thermogravimetric analyses. The thermogravimetry allows us to determine the V₂O₅ and H₂O content of the samples and rule out the presence of water in their stoichiometry (the decomposition of all the complexes starts above 300 °C). These complexes are isostructural with the bis chelated complexes formed by Hmpp, Hempp, Hppp, Hepp, Htp, Hpbb, and Hphp, which were prepared and characterized elsewhere.³¹ [V^{IV}O(dmpp)₂] was first studied by Burgess et al.³¹ and later by Buglyó et al.²⁸ Because it has not been possible to isolate single crystals suitable for an X-ray diffraction study, the characterization has been performed through spectroscopic (EPR and UV/vis) techniques. EPR and electronic absorption spectra were measured on the powders dissolved in several organic solvents (DMF, DMSO, and CH₃CN); the spectral data obtained in DMF are reported in Tables 4 and 5. To compare the data, we have re-examined the compounds studied previously³¹ in the present work, and all the spectra have been recorded and simulated in the same conditions.

In DMF, only the trans isomer is detected by EPR, supporting the weak coordinating properties of such a solvent. This is in agreement with the previous results obtained on [V^{IV}O(dmpp)₂].²⁸ The experimental spectrum of [V^{IV}O(depp)₂] in DMF is presented in Figure 5a. All the complexes exhibit A_z values (Table 4) closer to those displayed by bis chelated species formed by catechol and

Table 5. Electronic Absorption Parameters for Bis Chelated Solid V^{IV}O Complexes in DMF

complex	$\lambda_{IV}(\epsilon_{IV})^a$	$\lambda_{III}(\epsilon_{III})^a$	$\lambda_{II}(\epsilon_{II})^a$	$\lambda_I(\epsilon_I)^a$	$\Delta\lambda = (\lambda_{III} - \lambda_{II})^a$
[VO(mpp) ₂]	399(130)	540(60)	623(56)	695(25)	83
[VO(empp) ₂]	403(156)	547(57)	620(56)	699(15)	73
[VO(depp) ₂]	405(153)	546(62)	620(56)	700(21)	74
[VO(ppp) ₂]	402(188)	539(59)	624(48)	698(26)	85
[VO(epp) ₂]	402(145)	544(67)	619(60)	700(32)	75
[VO(ftp) ₂]	400(190)	541(69)	624(62)	699(30)	83
[VO(eftp) ₂]	401(165)	543(68)	618(63)	698(28)	75
[VO(pbp) ₂]	399(168)	538(73)	619(63)	697(25)	81
[VO(epbp) ₂]	404(170)	542(72)	620(64)	699(27)	78
[VO(php) ₂]	398(173)	538(65)	625(59)	698(26)	87
[VO(ephp) ₂]	403(178)	545(68)	621(61)	700(28)	76

^a λ measured in nanometers and ϵ in $\text{M}^{-1} \text{ cm}^{-1}$.

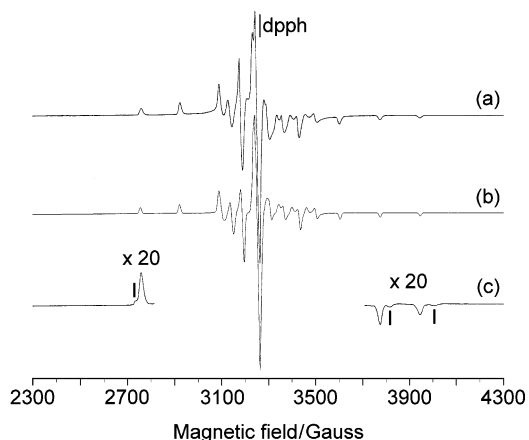


Figure 5. (a) Experimental and (b) simulated X-band anisotropic EPR spectrum recorded at 140 K on [V^{IV}O(depp)₂] dissolved in DMF. (c) Low- and high-field regions, amplified 20-fold, of the X-band anisotropic EPR spectrum recorded at 140 K on [V^{IV}O(depp)₂] dissolved in DMSO; **I** indicates the resonances of the *cis*-[V^{IV}O(depp)₂(dmsO)] complex. Diphenylpicrylhydrazyl (dpph) is the standard field marker ($g = 2.0036$).

3,4-dihydroxybenzoic acid ($A_z = 154\text{--}155 \times 10^{-4} \text{ cm}^{-1}$)⁴⁹ rather than by maltol ($A_z = 163 \times 10^{-4} \text{ cm}^{-1}$),^{14c} thus suggesting for pyridinones a (O^- , O^-) rather than a (CO , O^-) donor set. An x,y anisotropy ($g_x = 1.984\text{--}1.986$, $g_y = 1.977\text{--}1.978$, and $A_x = 45\text{--}46 \times 10^{-4} \text{ cm}^{-1}$, $A_y = 53\text{--}54 \times 10^{-4} \text{ cm}^{-1}$) is observed, comparable with that of [V^{IV}O-(maltolato)₂], for which a rhombic spectrum is detected in CH₂Cl₂ with a $|A_x - A_y|$ value of $9.3 \times 10^{-4} \text{ cm}^{-1}$.^{14c}

The electronic absorption spectra, measured in DMF, are similar for all the compounds and are characterized by four absorption bands in the visible region (Table 5 and Figure 6), with the low-energy transition (band I or λ_I) strongly shifted toward lower wavelengths with respect to aqua ion [V^{IV}O(H₂O)₅]²⁺ and with λ_I and λ_{II} values very close to each other. The deconvolution of the spectra is necessary to resolve band I, which otherwise appears as only a weak shoulder.

For a pentacoordinated complex of stoichiometry [V^{IV}OL₂], two geometries are conceivable: one close to the square-pyramid and another distorted toward the trigonal-bipyramid. The degree of distortion can be described by a structural index of trigonality, $\tau = (\beta - \alpha)/60$, where β is the angle subtended by vanadium between the two pseudo-apical donors and α the angle between the two pseudo-

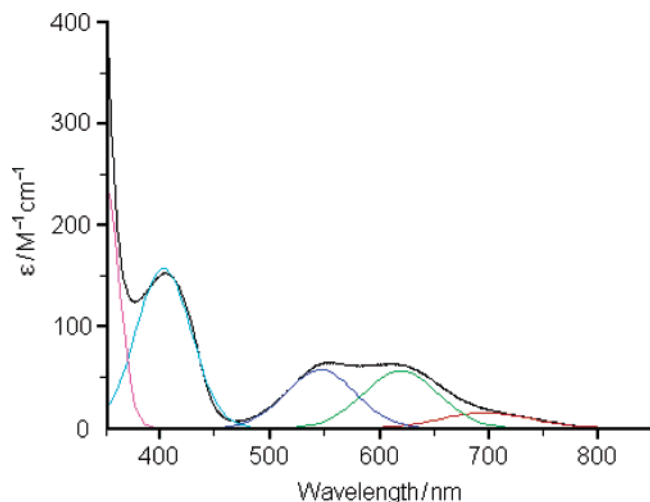
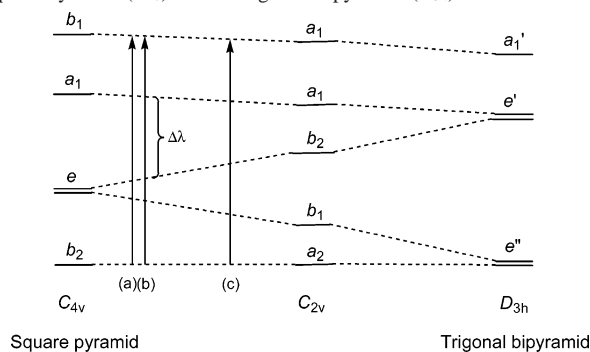


Figure 6. Electronic absorption spectrum recorded in DMF of $[\text{V}^{\text{IV}}\text{O}(\text{empp})_2]$ with a $\text{V}^{\text{IV}}\text{O}$ concentration of 0.25 mM. The colored curves, attributable to the four electronic transitions, have been obtained from the deconvolution of the spectrum.

Scheme 3. Orbital Correlation Diagram for the Transformation of a Square-Pyramid (C_{4v}) into a Trigonal-Bipyramid (D_{3h})^a



^a Arrows indicate the arbitrary distortion of $\text{V}^{\text{IV}}\text{O}$ complexes formed by (a) 2-methyl-3-hydroxy-4-pyridinones, (b) 2-ethyl-3-hydroxy-4-pyridinones and (c) α -hydroxycarboxylates.

equatorial donors ($\beta > \alpha$).⁵⁷ It was recently demonstrated that only the concurrent detection of rhombicity in the EPR and four transitions in the electronic absorption spectra is a criterion for proving a distortion of the $\text{V}^{\text{IV}}\text{O}$ complexes from a square-pyramidal toward a trigonal-bipyramidal geometry.^{6,7} This is due to the loss of degeneracy of the d_{xz} and d_{yz} atomic orbitals. In Scheme 3, the orbital correlation diagram calculated by Rossi and Hoffmann for the transformation of a square-pyramid into a trigonal-bipyramid is displayed.⁵⁸ In particular, the d_{xz} orbital (b_1 in C_{2v} symmetry) undergoes the greater stabilization. In the diagram, it can be noticed that, with increasing extent of the distortion, the λ_I band shifts to higher and λ_{II} to lower wavelengths. The λ_{III} and λ_{IV} bands undergo smaller changes. For severe distortions (Scheme 3c), $\lambda_I > 800$ nm and $\lambda_{II} < 600$ nm, as reported for the bis chelated species formed by α -hydroxycarboxylates;⁷ for example, for $[\text{V}^{\text{IV}}\text{O}(\text{benzilato})_2]^{2-}$, characterized by $\tau = 0.31$,⁵⁹ the λ_I and λ_{II} bands fall at 859 and 586 nm.⁷

For moderate distortions (a and b in Scheme 3), like those observed for $\text{V}^{\text{IV}}\text{O}$ pyridinonate complexes, intermediate values of λ_I and λ_{II} are expected, with λ_I in the range 695–700 nm and λ_{II} in the range 618–625 nm (Table 5). Finally, for square-pyramidal structures, λ_I and λ_{II} collapse into a single band observed between 650 and 700 nm; for $[\text{V}^{\text{IV}}\text{O}(\text{acetylacetonato})_2]$, for example, this band is detected at 675 nm in the solid, at 665 nm in CHCl_3 , and at 655 nm in benzene and toluene.⁶⁰ Thus, the detection of the low-energy band below 640–650 nm could suggest the presence of a unresolved band at higher wavelength and the probable distortion toward a trigonal-bipyramidal geometry.

Only a slight distortion is expected for bis chelated $\text{V}^{\text{IV}}\text{O}$ complexes formed by pyridinones in the light of the solid-state structures reported for $[\text{V}^{\text{IV}}\text{O}(\text{maltolato})_2]^{14a}$ and $[\text{V}^{\text{IV}}\text{O}(\text{catecholato})_2]^{2-}$,^{55a} close to the square-pyramid and characterized by very small values of τ (0.103 and 0.007, respectively). Therefore, the structure of $[\text{V}^{\text{IV}}\text{OL}_2]$ complexes is square-pyramidal with a very slight distortion toward the trigonal-bipyramid. The degree of such a distortion can be described by the splitting $\Delta\lambda$ between the two central bands (λ_{III} and λ_{II}) in the electronic spectra,⁷ related to the steric hindrance of the substituents on carbon atom in α -position to 3-hydroxy group, which favors the shift toward a trigonal-bipyramid arrangement.^{6,7} As can be seen in Scheme 3, the greater the distortion, the lower the $\Delta\lambda$ value. Analogously to what was observed for non-oxo complexes, the presence of the ethyl group ($\Delta\lambda = 73$ –78 nm, Scheme 3b) results in a bigger distortion with respect to that of methyl ($\Delta\lambda = 81$ –87 nm, Scheme 3a).

As a final comment, we would like to refer to the behavior of $[\text{V}^{\text{IV}}\text{OL}_2]$ complexes in DMSO (or CH_3CN). Both solvents have stronger coordinating ability than DMF and favor the partial isomerization of the $[\text{V}^{\text{IV}}\text{OL}_2]$ species with the formation of the cis isomer, in agreement with the results obtained for other ligands.⁴⁸ For example, in DMSO, both the *trans*- $[\text{V}^{\text{IV}}\text{OL}_2]$ and *cis*- $[\text{V}^{\text{IV}}\text{OL}_2(\text{dmsol})]$ isomers are observed (Figure 5c), and the relative amount of the cis species varies between 10 and 20%, depending on the ligand.

Discussion

The comparison of the present results with those reported for progressively stronger ligands, like kojic acid,⁴⁴ maltol,⁴⁴ L-mimosine,⁶¹ Hdmpp,²⁸ catechol,⁴⁹ and 3,4-dihydroxybenzoic acid (3,4-DHB),⁴⁹ allows us to infer some general features about the effect of the basicity and electronic structure on the thermodynamic (stability constants of the complexes) and spectroscopic (^{51}V hyperfine coupling constant) properties of $\text{V}^{\text{IV}}\text{O}$ species. Given the insulin-mimetic properties displayed by many of such systems, this could be useful for analyzing their biological behavior.

Even if, at first sight, it could seem that all these ligands are able to coordinate the $\text{V}^{\text{IV}}\text{O}$ ion in a similar way, a more careful analysis reveals that their complexing ability is very

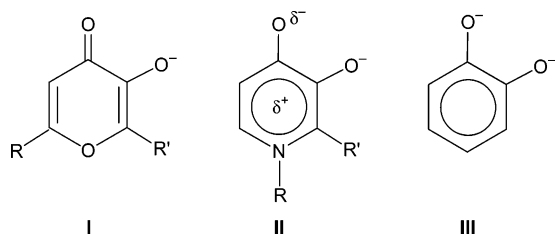
(57) Addison, A. W.; Rao, T. N.; Reedijk, J.; van Rijn, J.; Verschoor, G. C. *J. Chem. Soc., Dalton Trans.* **1984**, 1349–1356.

(58) Rossi, R.; Hoffmann, R. *Inorg. Chem.* **1975**, *14*, 365–374.

(59) Chasteen, N. D.; Belford, R. L.; Paul, I. C. *Inorg. Chem.* **1969**, *8*, 408–418.

(60) Selbin, J. *Chem. Rev.* **1965**, *65*, 153–175.

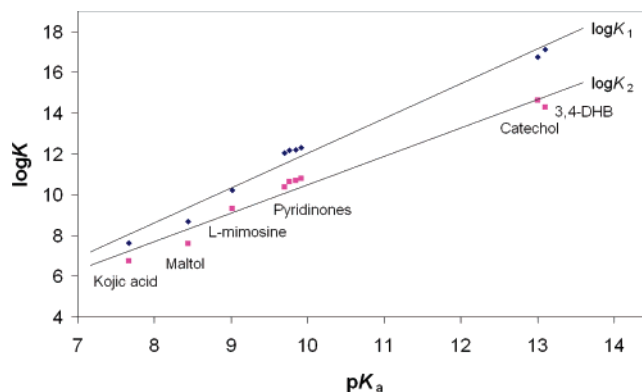
(61) Lodyga-Chruscinska, E.; Garribba, E.; Micera, G.; Panzanelli, A. *J. Inorg. Biochem.* **1999**, *75*, 225–232.

Scheme 4. Resonance Forms of Pyrone, Pyridinones, and Catechol Ligands

different and that pyrones, like kojic acid and maltol, are much weaker ligands than pyridinones and catechols, whereas L-mimosine shows an intermediate behavior. The combination of the inductive and resonance effects determines the following order of basicity: kojic acid < maltol < L-mimosine < pyridinones < catechol \approx 3,4-DHB. As suggested previously,^{21d,21e,22a} the contribution of the pseudo-aromatic form of the fully deprotonated ligands with both of the oxygen atoms of each ligand molecule negatively charged increases with increasing basicity (Scheme 4). When the characteristics of the donor set are compared, it is noticeable that this changes from that (CO, O⁻) typical of maltol and kojic acid (**I** in Scheme 4) to that (O⁻, O⁻) of catechol and 3,4-DHB (**III** in Scheme 4), with the intermediate form (O ^{δ^-} , O⁻) displayed by pyridinones lying between (**II** in Scheme 4). Therefore, it can be suggested that kojic acid and maltol exist almost exclusively in form **I** in Scheme 4, whereas catechol and 3,4-DHB exist in form **III**. L-mimosine and pyridinone derivatives should show an intermediate electronic structure with a partial negative charge on the oxygen atom in position 4 and a pseudo-aromatic configuration of the six-membered ring.

These findings are confirmed by the analysis of the X-ray solid structures of [V^{IV}O(maltolato)₂]²⁺^{2a} and [V^{IV}O-(catecholato)₂]²⁻.^{55a} To establish the predominance of the resonance forms **I** or **III**, we could introduce two structural parameters, $\Delta d(\text{V}-\text{O}) = [d(\text{V}-\text{O}(\text{keto})) - d(\text{V}-\text{O}(\text{hydroxy}))]$ and $\Delta d(\text{C}-\text{O}) = [d(\text{C}-\text{O}(\text{hydroxy})) - d(\text{C}-\text{O}(\text{keto}))]$, related to the asymmetry of the V–O(keto) and V–O(hydroxy) on one hand, and C–O(keto) and C–O(hydroxy) distances on the other hand. The larger the values of $\Delta d(\text{V}-\text{O})$ and $\Delta d(\text{C}-\text{O})$, the greater the contribution of form **I**. $\Delta d(\text{V}-\text{O})$ and $\Delta d(\text{C}-\text{O})$ are 0.046 and 0.080 Å for [V^{IV}O-(maltolato)₂]^{14a} and 0.013 and 0.007 Å for [V^{IV}O-(catecholato)₂]²⁻,^{55a} in good agreement with the hypothesis illustrated in Scheme 4.

The stepwise stability constants (log K_1 and log K_2) for the formation of mono and bis chelated complexes of pyridinones through the reactions VO + L \rightarrow VOL and VOL + L \rightarrow VOL₂ (log K_1 = 12.05–12.30 and log K_2 = 10.37–10.80, Table 1) are about 3 and 4 orders of magnitude bigger than for maltol (log K_1 = 8.69 and log K_2 = 7.60)⁴⁴ and kojic acid (log K_1 = 7.63 and log K_2 = 6.74)⁴⁴ and about two orders of magnitude bigger than for L-mimosine (log K_1 = 10.21 and log K_2 = 9.31).⁶¹ Catechol and 3,4-DHB can be considered the final terms of the series, and their stepwise stability constants are about 4 orders of magnitude greater than those of pyridinones (log K_1 = 16.75 and log

**Figure 7.** Stepwise stability constants (log K_1 and log K_2) of the mono and bis chelated complexes formed by the discussed ligands as a function of the pK_a values of the –OH group. Values are taken from refs 28, 44, 49, 61, and from this work.

K_2 = 14.63 for catechol, and log K_1 = 17.13 and log K_2 = 14.29 for 3,4-DHB).⁴⁹ The above results show that pyridinones have an intermediate coordinating strength with respect to maltol and catechol. In Figure 7, the stepwise stability constants for mono and bis chelated complexes (log K_1 and log K_2 , respectively) formed by a number of pyrones, pyridinones, and catechols are represented as a function of the pK_a values of –OH group in position 3 of the six-membered ring.

In Figure 7, a linear relationship between the basicity of the ligands and the stepwise stability constants of the V^{IV}O complexes is observed. Greater values of stability constants are expected for complexes of more basic ligands, as has already often been reported in the literature, for example, for substituted pyridine derivatives.⁶²

With increasing basicity of the ligands, an increased tendency to stabilize the trans arrangement of the four donors with respect the V=O bond is observed. Indeed, bis complexes formed by kojic acid and maltol are present in aqueous solution only as cis isomers with one of the two ligand molecules in an (equatorial–axial) arrangement;^{14a,14c,16a,44} L-mimosine forms mainly the cis isomer, but a small amount of the trans isomer is detected.⁶¹ With pyridinones, the trans complex prevails over the cis,²⁸ whereas with catechol and 3,4-DHB only the trans species exist in water.⁴⁹ The experimental EPR spectra for the latter four cases are displayed in Figure 8.

These results are confirmed by EPR spectroscopy and potentiometry, which suggest a *cis*-V^{IV}OL₂H₋₁ species, formed upon deprotonation of the equatorially coordinated water molecule, in all the systems except in those with catechol and 3,4-DHB. By proceeding from the weakest ligand (kojic acid) to the strongest (Hdepp), the pK of the water in the equatorial plane of V^{IV}O ion increases progressively: values of 8.46 (kojate),⁴⁴ 8.78 (maltolate),⁴⁴ 9.22 (L-mimosinate),⁶¹ and 10.59 (Hdmpp)²⁸ are reported in the literature. The pK values measured in this work lie in the range 10.47–10.75 (Table 1). The bis chelated V^{IV}OL₂ complexes are stabilized by stronger ligands and the formation of *cis*-V^{IV}OL₂H₋₁ species is shifted to higher pH values.

(62) Kapinos, L. E.; Sigel, H. *Inorg. Chim. Acta* **2002**, 337, 131–142.

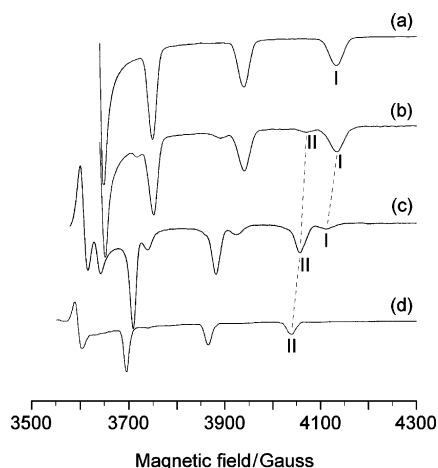


Figure 8. Low-field region of the X-band anisotropic EPR spectra of the bis chelated complexes formed by maltol, L-mimosine, Hdepp, and catechol recorded in aqueous solutions at 140 K with $V^{IV}O$ concentration of 4 mM. (a) Maltol: L:M = 4, pH 5.50. (b) L-Mimosine: L:M = 5, pH 5.25. (c) Hdepp: L:M = 3, pH 6.00. (d) Catechol: L:M = 2, pH 5.00. I and II denote the *cis*- $V^{IV}OL_2$ and *trans*- $V^{IV}OL_2$ complexes, respectively.

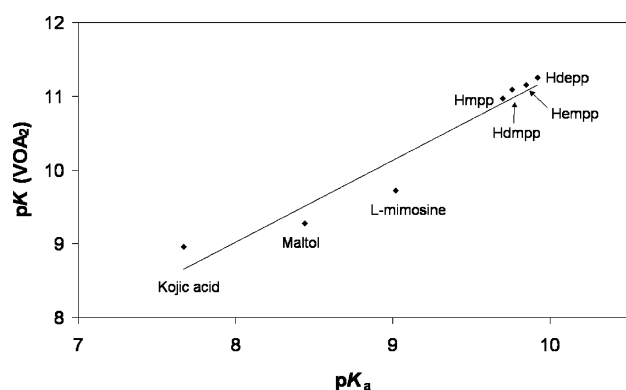


Figure 9. pK of the equatorial water molecule in the bis chelated *cis*- $V^{IV}OL_2$ complexes formed by the discussed ligands as a function of the pK_a values of the $-OH$ group. Values are taken from refs 28, 44, 61, and from this work.

In Figure 9, the relationship observed between the pK_a of the $-OH$ group in the free ligand and the pK of the equatorial water molecule coordinated in *cis* position with respect to the $V=O$ bond is presented.

An analogous trend is found for the formation of the $V^{IV}L_3$ non-oxo species through reaction 1. The value of $\log K$ can be calculated by the equation $\log K(VL_3 \cdot H_2O) = \log \beta(VL_3 \cdot H_2O) - \log \beta(VOL_2) - \log \beta(HL)$. In this case, the comparison concerns a number of catechol derivatives, like tiron,⁶³ dopamine, D,L-epinephrine, D,L-norepinephrine, and L-dopa.⁵⁰ Pyridinones, the weakest ligands of the series, show a decreased ability to form non-oxo tris chelated complexes, as is demonstrated by the distribution diagram shown in Figure 1. In Figure 10, $\log K(VL_3 \cdot H_2O)$ is plotted as a function of the pK_a of the $-OH$ group.

The value of the hyperfine coupling constant along the z axis of the unpaired electron with the ^{51}V nucleus (A_z) can be calculated from the sum of the contribution of each donor function in the equatorial plane, according to the additivity

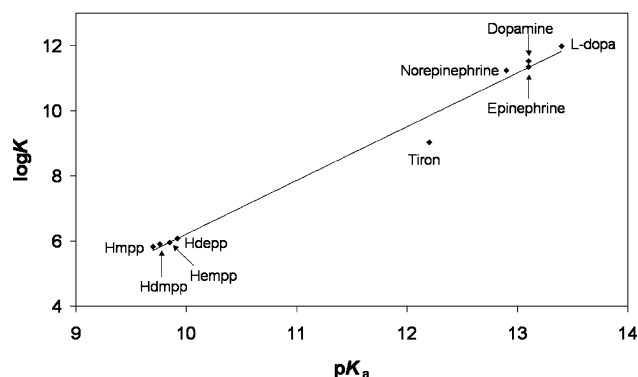


Figure 10. Stability constants ($\log K$) of the non-oxo tris chelated complexes $V^{IV}L_3$ formed by the discussed ligands as a function of the pK_a values of the $-OH$ group. Values taken from refs 28, 50, 63, and from this work.

relationship proposed first by Wütrich⁶⁴ and subsequently developed by Chasteen⁴⁵

$$A_z = \sum_{i=1}^4 A_z(i) = A_z(\text{donor 1}) + A_z(\text{donor 2}) + A_z(\text{donor 3}) + A_z(\text{donor 4}) \quad (2)$$

Recently, the list of the donor atoms was completed by Tolis et al. for Cl^- and SCN^- ions,⁶⁵ by Hamstra et al. for a neutral oxygen atom belonging to an amide CO group,⁶⁶ by Cavaco et al.⁶⁷ and Garribba et al.⁶⁸ for the imino nitrogen atom, and by Tasiopoulos et al.⁶⁹ and Garribba et al.⁶⁸ for the deprotonated amide nitrogen. Corrections to the contribution of the carboxylate group and the imidazole nitrogen that is dependent on the orientation of the aromatic ring with respect to the $V=O$ bond were proposed by Jakusch et al.⁷⁰ and Smith II et al., respectively.⁷¹

Usually, the contribution to A_z is considered constant for each donor function (for example, that for the $Ph-O^-$ group is always $38.9 \times 10^{-4} \text{ cm}^{-1}$),⁴⁵ without considering the possible change in its basicity due to different substituents in the ligand molecule. With the values reported for the $A_z(Ph-O^-)$ ⁴⁵ and $A_z(C=O)$ groups,⁶⁶ the expected hyperfine coupling constants for $[V^{IV}O(\text{maltolato})_2]$ ($\sim 165 \times 10^{-4} \text{ cm}^{-1}$) and $[V^{IV}O(\text{catecholato})_2]^{2-}$ ($\sim 156 \times 10^{-4} \text{ cm}^{-1}$) are easily calculated; the experimental values are $163 \times 10^{-4} \text{ cm}^{-1}$ ^{14c} and $154 \times 10^{-4} \text{ cm}^{-1}$.^{49,54} The results obtained in this work allow us to establish how the hyperfine coupling

(64) Wütrich, K. *Helv. Chim. Acta* **1965**, *48*, 1012–1017.

(65) Tolis, E. J.; Teberkidis, V. I.; Raptopoulou, C. P.; Terzis, A.; Sigalas, M.; Deligiannakis, Y.; Kabanos, T. A. *Chem.—Eur. J.* **2001**, *7*, 2698–2710.

(66) Hamstra, B. J.; Houseman, A. P. L.; Colpas, G. J.; Kampf, J. W.; LoBrutto, R.; Frisch, W. D.; Pecoraro, V. L. *Inorg. Chem.* **1997**, *36*, 4866–4874.

(67) Cavaco, I.; Costa Pessoa, J.; Costa, D.; Duarte, M. T.; Gillard, R. D.; Matias, P. J. *Chem. Soc., Dalton Trans.* **1994**, 149–157.

(68) Garribba, E.; Lodyga-Chruscinska, E.; Micera, G.; Panzanelli, A.; Sanna, D. *Eur. J. Inorg. Chem.* **2005**, 1369–1382.

(69) Tasiopoulos, A. J.; Troganis, A. N.; Evangelou, A.; Raptopoulou, C. P.; Terzis, A.; Deligiannakis, Y.; Kabanos, T. A. *Chem.—Eur. J.* **1999**, *5*, 910–921.

(70) Jakusch, T.; Buglyó, P.; Tomaz, A. I.; Costa Pessoa, J.; Kiss, T. *Inorg. Chim. Acta* **2002**, *339*, 119–128.

(71) Smith, T. S., II; Roof, C. A.; Kampf, J. W.; Rasmussen, P. G.; Pecoraro, V. L. *J. Am. Chem. Soc.* **2000**, *122*, 767–775.

(63) Buglyó, P.; Kiss, T. *J. Coord. Chem.* **1991**, *22*, 259–268.

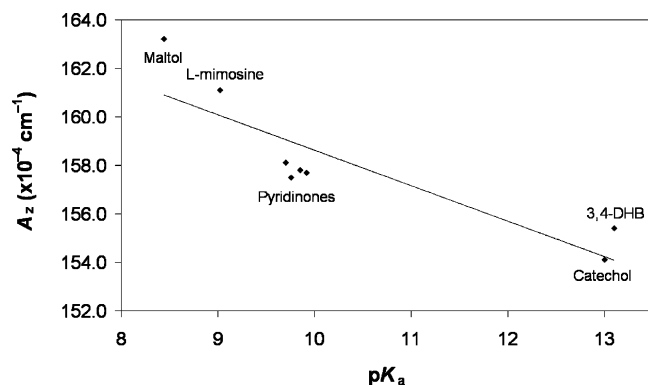


Figure 11. Hyperfine coupling constant value, A_z , for the bis chelated $trans$ -V^{IV}OL₂ complexes formed by the discussed ligands as a function of the pK_a values of the $-OH$ group. Values are taken from refs 14c, 28, 49, 54, and from this work.

constant change for the $trans$ bis chelated complexes in the transformation of the donor set from maltol to catechol. For L-mimosine and pyridinone derivatives, it would be incorrect to calculate the A_z value from the data reported in the literature,^{45,66} because the oxygen donor in position 4 of the pseudo-aromatic ring exhibits a chemical behavior intermediate with respect to the two limiting cases **I** and **III** in Scheme 4. Interestingly, $trans$ -V^{IV}OL₂ complexes formed by L-mimosine and pyridinones are characterized by A_z values of $161 \times 10^{-4} \text{ cm}^{-1}$ and $158\text{--}159 \times 10^{-4} \text{ cm}^{-1}$, respectively, intermediate between those of pyrones and catechols. The decrease in the A_z value is evident in Figure 8. A similar trend is observed for cis -V^{IV}OL₂(H₂O) species (Figure 8): from maltol to pyridinones, A_z changes from $171 \times 10^{-4} \text{ cm}^{-1}$ ^{14c,44} to $166\text{--}167 \times 10^{-4} \text{ cm}^{-1}$.²⁸ Analogously, A_z is $167 \times 10^{-4} \text{ cm}^{-1}$ for the hydrolytic cis -V^{IV}OL₂(OH) species formed by maltol,⁴⁴ and $161\text{--}162 \times 10^{-4} \text{ cm}^{-1}$ for those formed by pyridinones. In Figure 11, the experimental values of the hyperfine coupling constant, A_z , are represented as a function of the pK_a of the $-OH$ group.

Conclusions

Eleven derivatives of 3-hydroxy-4-pyridinones coordinate a V^{IV}O ion at 1:2 metal:ligand molar ratios in the pH range 2–12 with the formation of complexes with [V^{IV}OL]⁺, [V^{IV}-OL₂], [V^{IV}OL₂H₋₁]⁻, [(V^{IV}O)₂L₂H₋₂], and [V^{IV}L₃]⁺ stoichiometries. The additivity rule allows us to identify the donors coordinated in the equatorial plane of the V^{IV}O ion.⁴⁵ Bis chelated species are characterized by a cis – $trans$ isomerism, with the $trans$ arrangement strongly favored with respect to the cis one. The presence of the cis isomer is displayed by potentiometric titrations, which show a deprotonation process in the pH range 10–11, and by EPR spectroscopy. Cis – $trans$ equilibrium now appears to be a general behavior of V^{IV}O complexes.^{5,44,47,48}

Tris chelated species are not very stable in aqueous solution, but can be synthesized in concentrated CH₃COOH, which allows for the cleavage of the V=O bond with formation of a water molecule. As observed for V^{IV} complexes of catechol derivatives,^{49,54} they are characterized

by a d_z^2 ground state and by a geometry that can be described as being intermediate between the octahedron and the trigonal prism.

The donor set is intermediate between that of maltol (CO, O⁻) and catechol (O⁻, O⁻) and shows a partial negative charge on the oxygen atom in position 4 and a pseudo-aromatic electronic configuration of the six-membered pyridinone ring. These features seem to explain the increased coordinating strength of pyridinones in comparison with those exhibited by simple pyrone derivatives.

The characterization of the solid derivatives, [V^{IV}O-(depp)₂], [V^{IV}O(ept)₂], [V^{IV}O(epbp)₂], and [V^{IV}O(ephp)₂], was performed through EPR and UV/vis spectroscopies and the structure is close to the square-pyramid, according to the previous results.³¹ The detection of four bands in the electronic spectra and rhombicity in the EPR spectra in DMF suggest a slight distortion toward the trigonal-bipyramid.^{6,7} A structural index of trigonality τ between those of [V^{IV}O-(maltolato)₂] (0.103)^{14a} and [V^{IV}O(catecholato)₂]²⁻ (0.007)^{55a} could be expected. A criterion for establishing the degree of distortion is the position of bands I (λ_I) and II (λ_{II}) in the electronic absorption spectrum: if $\lambda_I > 800 \text{ nm}$ and $\lambda_{II} < 600 \text{ nm}$, the distortion is severe, as for bis chelated species formed by α -hydroxycarboxylates;⁷ if $\lambda_I \approx 700 \text{ nm}$ and $\lambda_{II} \approx 600\text{--}620 \text{ nm}$, the distortion is moderate, as happens with pyridinones. It must be noticed that for moderate distortions, band I could be unresolved; in such cases, the position of the low-energy observable band (band II) below 640–650 nm should suggest a trigonal-bipyramidal distortion and a deconvolution of the experimental spectrum is advisable to resolve band I.

A comparison with other pyrone, pyridinone, and catechol ligands^{14a,14c,28,44,49,50,61,63} shows that, with an increase in the pK_a value of the $-OH$ group in position 3 of the ring, there is an increase in (i) stepwise stability constants ($\log K_1$ and $\log K_2$) of the mono and bis chelated complexes, (ii) the pK of the equatorial water molecule in cis -V^{IV}OL₂(H₂O), and (iii) $\log K$ of the non-oxo tris chelated complexes V^{IV}L₃, whereas there is a decrease in (iv) ⁵¹V hyperfine coupling constant A_z . From these data, we can predict the relative stability of the $trans$ and cis isomers in terms of the basicity and electronic structure of the ligands. In particular, in aqueous solution, kojic acid and maltol form only cis complexes,^{14a,14c,16a,44} L-mimosine almost exclusively the cis species,⁶¹ pyridinones mainly the $trans$ isomer,²⁸ and catechols only the $trans$ complexes.^{49,55a}

Supporting Information Available: Tables S1 and S2 giving the protonation constants of the ligands (pK_a) and stability constants of V^{IV}O complexes ($\log \beta$) formed by pyrone, pyridinone, and catechol ligands reported in the literature. Figures S1 and S2 showing the electronic absorption spectra of [V^{IV}(empp)₃]⁺ and [V^{IV}(mpp)₃]⁺ in CH₃COOH and [V^{IV}O(mpp)₂] and [V^{IV}O(depp)₂] in DMF. This material is available free of charge via the Internet at <http://pubs.acs.org>.

IC0605571